

Original Article

Combination of melatonin-delivered endothelial progenitor cells with S-nitroso-N-acetyl-DL-penicillamine for improving critical limb ischemia in the rat

Jui-Ning Yeh^{1*}, Hon-Kan Yip^{2,3,4,5,6*}, Pei-Lin Shao⁵, John Y Chiang^{7,8}, Shun-Cheng Wu^{9,10,11}, Pei-Hsun Sung^{2,3,4}, Jiunn-Jye Sheu^{2,3,12}, Jun Guo¹

¹Department of Cardiology, The First Affiliated Hospital, Jinan University, Guangzhou 510630, Guangdong, China; ²Division of Cardiology, Department of Internal Medicine, Kaohsiung Chang Gung Memorial Hospital, Chang Gung University College of Medicine, Kaohsiung 83301, Taiwan; ³Center for Shockwave Medicine and Tissue Engineering, Kaohsiung Chang Gung Memorial Hospital, Kaohsiung 83301, Taiwan; ⁴Institute for Translational Research in Biomedicine, Kaohsiung Chang Gung Memorial Hospital, Kaohsiung 83301, Taiwan; ⁵Department of Nursing, Asia University, Taichung 41354, Taiwan; ⁶Department of Medical Research, China Medical University Hospital, China Medical University, Taichung 40402, Taiwan; ⁷Department of Computer Science and Engineering, National Sun Yat-Sen University, Kaohsiung 80424, Taiwan; ⁸Department of Healthcare Administration and Medical Informatics, Kaohsiung Medical University, Kaohsiung 80708, Taiwan; ⁹Regenerative Medicine and Cell Therapy Research Center, Kaohsiung Medical University, Kaohsiung 80787, Taiwan; ¹⁰Orthopaedic Research Center, Kaohsiung Medical University, Kaohsiung 80787, Taiwan; ¹¹Post-Baccalaureate Program in Nursing, Asia University, Taichung 41354, Taiwan; ¹²Division of Thoracic and Cardiovascular Surgery, Department of Surgery, Kaohsiung Chang Gung Memorial Hospital and Chang Gung University College of Medicine, Kaohsiung 83301, Taiwan. *Equal contributors.

Received October 18, 2023; Accepted February 10, 2024; Epub September 15, 2024; Published September 30, 2024

Abstract: Background: This study tested whether combined shock wave (SW)-facilitated melatonin (Mel) delivered into endothelial progenitor cells (EPCs) (EPC^{SW-Mel}) plus S-nitroso-N-acetyl-DL-penicillamine (SNAP) was superior to merely one modality alone for improving critical limb ischemia (CLI) in rats. Methods: SD rats (n = 50) were equally categorized into group 1 (sham-control), group 2 (CLI), group 3 (CLI + SNAP), group 4 (CLI + EPC^{SW-Mel}), and group 5 (CLI + EPC^{SW-Mel} + SNAP), and ischemia-involved quadriceps were harvested by day 14. Results: An in vitro study showed that at time points of 24/48/72 h, the cell viability/protein expression of endothelial nitric oxide synthase (eNOS)/and cellular expression of nitric oxide (NO) were highest in EPCs, lowest in EPCs + menadione, and much higher in EPC^{SW-Mel} + Mena than in EPCs + Mena + Mel. Protein levels of oxidative-stress (NOX-1/NOX-2/oxidized protein)/early (AN-V⁺/PI⁻)/late (AN-V⁺/PI⁺) apoptosis and total intracellular/mitochondrial reactive oxygen species ROS exhibited an antithetical trend of cell viability among the groups (all P<0.0001). Matrigel assay of angiogenesis/positively-stained NO cells showed that they were much higher in EPCs + SNAP than in EPCs only (all P<0.0001). Ex vivo angiogenesis/arterial relaxation of carotid-artery rings were highest in left-common-carotid-artery (LCCA) + SNAP, lowest in LCCA + Mena, and notably higher in LCCA than in LCCA + Mena + SNAP (all P<0.0001). Laser Doppler showed ischemic to normal-blood-flow (INBF) ratio was highest in group 1, lowest in group 2, and it progressively increased from groups 3 to 5 (all P<0.0001). The protein levels of oxidative-stress (NOX-1/NOX-4/oxidized protein)/apoptotic [cleaved-caspase-3/cleaved apoptosis/mitochondrial-damage (cytosolic-cytochrome-C/p-DRP-1)]/fibrotic (Smad3/TGF-β)/inflammatory (MMP-9/IL-1β/TNF-α/NF-κB) biomarkers, exhibited an opposite trend, whereas the protein level of endothelial-cell surface markers (CD31/vWF/eNOS) and number of small vessels exhibited an identical pattern of INBF ratio among the groups (all P<0.0001). Conclusions: Combined EPC^{SW-Mel} and SNAP therapy offered a synergic effect toward rescuing from CLI.

Keywords: Critical limb ischemia, nitric oxide donor, angiogenesis, endothelial progenitor cells, shock wave, melatonin

Introduction

Peripheral arterial occlusive disease (PAOD) affects an estimated 20 to 27 million people globally [1-5]. Limb ischemia (LI), defined as [1-5] ischemic rest painful sensation, ischemic ulcerations, or presence of ischemic gangrene change, represents the most critical manifestation of PAOD and is correlated with unfavorable cardiovascular and peripheral vascular clinical outcome [1-5].

Without aggressive and effective management, PAOD frequently evolves into chronic limb-threatening ischemia (CLTI) or promptly into more worsening stage, called critical LI (CLI) (i.e., the end stage of PAOD) [1, 3, 4, 6-8]. In this way, CLI, defined as limb ischemia symptoms for longer than 2 weeks, is characterized by a cascade of significantly hemodynamically macrovascular arteriosclerotic obstruction and microvascular ischemic changes, resulting in markedly reduced tissue/muscle perfusion and oxygen supply, interrupted muscle energy metabolism and functional integrity, and generations of inflammatory reaction and abundant oxidative stress/free radicals [5, 8, 9]. Clearly, lower extremity of CLI represents symptoms related to end-stage atherosclerotic PAOD manifested by rest pain and severe ischemia and tissue loss [10]. Undoubtedly, this commonly carries a high risk of limb amputation, impaired quality of life, and cardiovascular-related morbidity and mortality [5, 10-12].

CLI treatment remains a tough challenge to internal medicine and surgeons [5, 8, 9, 12, 13]. Without an appropriate and prompt treatment, an estimated one-year mortality rate has been reported to be as high as 22% [13]. Guidelines have recommended that except for antiplatelet agents, catheter-based endovascular interventions (i.e., by either balloon angioplasty and stenting) and bypass surgery are two standard modalities for treatment of CLTI/CLI [14]. However, the amputation-free and overall survival rate are still relatively low [3, 8, 9, 11, 15], especially in those with end-stage renal disease [12]. Accordingly, as the number of patients afflicted by PAOD, and CLTI/CLI continue to grow, new and innovative solutions are necessary to furnish effective and durable treatment options that will lead to improved outcomes.

It is well recognized that nitric oxide (NO), which is mainly released by endothelial cells in the arteries is the most potent intrinsic vasodilator. NO plays a crucial role on arterial venous dilatation, anti-thrombosis, and angiogenesis, and has the capacity of increasing small vessel/capillary permeability for endothelial progenitor cells (EPCs) from circulation migrating into tissue, especially in the ischemic areas for angiogenesis/neovascularization, resulting in restoration of blood flow to the ischemic area. However, in CLI patients, the arteries always progressively develop severe occlusive arteriosclerosis along with obvious endothelial dysfunction, resulting in extremely inadequate NO generation and limiting the migration of circulatory EPCs into the ischemic area for angiogenesis [16, 17]. Additionally, in the setting of CLI, the oxidative stress, reactive oxygen species (ROS), hypoxic conditions, and free radicals are always increased and the generations of proinflammatory cytokines and inflammatory cell infiltration are enhanced in the ischemic area [18-20]. In this way, even some circulatory EPCs can migrate into the ischemic area. However, they would always have a very short survival time due to the impact of such an unsuitable environment. These aforementioned issues may explain why the majority of clinical trials of autologous bone marrow mononuclear cells/EPCs treatment for PAOD have failed [21-27]. Thus, enforcing a longer survival rate and functional integrity of EPCs may be the first step for successful cell therapy of limb ischemia.

Evidence has shown that melatonin (Mel), a potent free radical scavenger, has capacities for antioxidant stress and anti-inflammation, and serves as mitochondrial protector [28-33]. Additionally, Mel therapy ensures cell survival in a toxic environment through inhibiting the generation of ROS and oxidative stress [30]. Furthermore, our recent study has shown that extracorporeal shock wave (ECSW) could facilitate exogenous mitochondria and cancer drug incorporation into target cells, which has been utilized for successful treatment of acute respiratory distress syndrome (ARDS) [34] and tongue squamous cell carcinoma [35]. Thus, we believe that ECSW can augment Mel uptake into EPCs for more enhancement of EPC resistance to oxidative-stress/ROS-induced damage to EPCs in the ischemic area. Moreover, S-nitroso-N-acetyl-DL-penicillamine (SNAP), a

Endothelial progenitor cells and SNAP for limb ischemia

NO donor, has been revealed to effectively control the release of NO from various biomaterials and the nervous system under physiologic conditions [36-39].

Based on the above-mentioned issues, it is reasonable to believe that combined SNAP and ECSW-facilitated delivery of Mel into EPC therapy may effectively rescue the CLI in rats.

Materials and methods

Ethical issues

The formalities of animal studies were authorized by the Committee at Kaohsiung Chang Gung Memorial Hospital (Affidavit of Approval of Animal Use Protocol No. 2022031103), followed the Guide for the Care and Use of Laboratory.

Cell grouping

The rat circulatory endothelial progenitor cells (EPCs) were categorized into group A1 (EPCs only), group A2 [EPCs (1.0×10^5 cells) + menadione (Mena) (25 μ M) co-cultured for 6 h], group A3 [EPCs (1.0×10^5 cells) + Mena (25 μ M) co-cultured for 6 h + melatonin (Mel) (100 μ M) co-cultured for 24 h], and group A4 [applied ECSW (0.14 mJ/mm²) for 120 shots to Mel (100 μ M) treated EPCs (i.e., EPC^{SW-Mel}) followed by 24 h co-culture + Mena (25 μ M) co-cultured for first 6 h]. Additionally, the rat circulatory EPCs were categorized into group B1 (EPCs only), and group B2 [SNAP (100 μ M) co-cultured with EPCs for 24 h]. The dosages of Mena [40], Mel [30, 32], and ECSW [34] energy was based on our previous reports [30, 32, 34, 40]. The purposes of these cell groupings were utilized for individual study and the results are illustrated in the **Figures 2 and 3**.

Ex vivo carotid artery culture for determining carotid angiogenesis

For the assessment of *ex vivo* angiogenesis, we used Sprague-Dawley (SD) rat carotid ring passing through culture and this *ex vivo* study was categorized into 5 groups as: group A [left common carotid artery (LCCA only)], group B [LCCA + SNAP (100 μ M) incubated for 24 h, followed by culturing for 5 days], group C [LCCA + Mena (25 μ M) co-cultured for 6 h, followed by continuous culturing for 5 days] and group D [LCCA + Mena (25 μ M) co-cultured for 6 h, followed by

SNAP (100 μ M) incubated for 12 h, and then continuously cultured for 15 days], respectively.

Peripheral blood-derived mononuclear cells (PBMNCs) isolation and EPC culture

The methodologies were based on our previous study [41]. Briefly, after 3 cc peripheral blood sampling (i.e., from one animal), PBMNCs were isolated by density gradient centrifugation using a Ficoll gradient without brake. Additionally, the PBMNC layer was isolated by centrifugation without brake and washed with PBS several times. The PBMNCs were then cultured with the endothelial growth medium-2 (EGM-2; Clonetics®, CA, USA) on the fibronectin-coated dish at 37°C with 5% CO₂ and the culture medium was changed every 48 h. The final product was designated EPCs. By day 21, cells with a cobblestone-like phenotype typical of endothelial cells (i.e., about 2.0 to 3.0×10^6 cells from about 3.0 cc PBMNCs) were found attached to the plate.

Autologous EPCs were utilized for the animals. Thus, the circulatory blood samplings were collected by day 21 prior to CLI induction.

Investigation of LCCA contractility, vasorelaxation, and NO release

For the purpose of this study, an additional six rats served as donors for donating the LCCA to be harvested, cleaned, and cut into slices of 2 mm in length for evaluating contractile and relaxant responses as in our previous report [30]. The carotid rings were carefully mounted on an isometric force transducer with a tension of 1.8 g and placed in an organ chamber filled with Krebs solution maintained at pH 7.4 and bubbled with 95% O₂ and 5% CO₂. After an equilibration of 40 minutes, 1 μ M of phenylephrine (PE) was added to the organ chamber for the assessment of contractile activity, and then 30 μ M of acetylcholine (Ach) was added to assess endothelial integrity. All data were acquired and analyzed using the Danish Myo Technology (DMT, i.e., DMT dual wire myograph system) system for analysis.

Vascular basal NO release was calculated as the percentage difference between PE-induced vasocontractile response in the presence and absence of L-NAME, as previously described [30].

Endothelial progenitor cells and SNAP for limb ischemia

Assessment of rat aortic-ring angiogenesis

The methodology was based on our recent reports [30]. In detail, rat aortic ring angiogenesis was assessed in 24-well tissue culture plates which were embedded with 150 μ L of 1 mg/mL type I collagen (BD Biosciences, Franklin Lakes, NJ, USA) and allowed to gel for 60 minutes at 37°C and 5% CO₂. The aorta was then cut into 1 mm cross-section pieces, and placed in collagen-coated wells before filling with 500 μ L of serum-free MCDB131 medium. The aortic rings were incubated for 5 days at 37°C and 5% CO₂. Photographs were taken on the first day and at the day 15 with 12.5 \times magnification. The number and length of sprouting vessels were quantified by ULYMPUS DP72 software.

Matrigel assay for evaluating EPC angiogenesis

The protocol and procedure for assessing angiogenesis were performed as reported in our previous reports [30, 41]. The EPCs were plated in 96-well plates at 1.0×10^4 cells/well in 150 μ L serum-free M199 culture medium mixed with 50 μ L cold Matrigel (Chemicon International, Inc., Temecula, CA, USA) for 24 h using passage 3 to 4 EPCs incubated at 37°C in 5% CO₂. Three random microscopic images (200 \times) were taken from each well to count cluster, tube, and network formations, and the mean values were obtained.

Flow cytometric analysis for assessment of total intracellular and mitochondrial ROS production and apoptosis

Carboxy-H₂DCFDA (Invitrogen, Life Technologies, Carlsbad, CA, USA) was used for assessment of total intracellular ROS generation. The carboxy-H₂DCFDA dye was diluted in PBS at a concentration of 10 μ M and the plates were kept in a 37°C, 5% CO₂ incubator for 30 minutes. For investigation of mitochondrial ROS in the cells, the MitoSOX™ Red dye was directly added at a concentration of 10 nM for an additional 30 min. incubation. Fluorescence intensity was analyzed with Beckman Coulter Cytomics FC 500 Flow Cytometer.

The percentages of viable and apoptotic cells were determined by flow cytometry using double staining of annexin V and propidium iodide

(PI) as our previous report [30]. The early (annexin V⁺/PI⁻) and late (annexin V⁺/PI⁺) phases of cell apoptosis were analyzed.

Animal model of CLI, animal grouping, and measurement of blood flow with laser Doppler

The procedure and protocol were based on our previous report [30]. Briefly, animals were anesthetized by inhalation of isoflurane (2.0%) prior to CLI induction and at days 1, 7, 14 after CLI induction prior to sacrifice. The rats were placed supine on a warming pad (37°C) and blood flow was detected in both inguinal areas by a laser Doppler scanner (moorLDLS, Moor Instruments, UK). The ratio of flow in the left (ischemic) leg and right (normal) leg was computed. On day 14, the animals were euthanized, and the quadriceps muscle was collected for individual study.

Animals (n = 50) were equally categorized into group 1 [Sham-operated control (SC)], group 2 (CLI only), group 3 [CLI + SNAP (1.0 mg/kg) by intramuscular injection at 3 h after CLI induction], group 4 [CLI + ECSW facilitated Mel (100 μ M) delivery into autologous EPCs (1.2×10^6 cells) (EPC^{SW-Mel}), followed by intramuscular injection at 3 h after CLI induction], and group 5 [CLI + (EPC^{SW-Mel}) + SNAP (1.0 mg/kg) followed by intramuscular injection at 3 h after CLI induction], respectively. By day 14 after CLI procedure, the animals in each group were sacrificed and the quadriceps muscle from the ischemic area was harvested for individual study.

Western blot analysis

The procedure and protocol for western blot analysis were based on our previous reports [16-20, 30]. Briefly, equal amounts (50 μ g) of protein extracts were separated by SDS-PAGE. After electrophoresis, the separated proteins were transferred onto a polyvinylidene difluoride (PVDF) membrane (Amersham Biosciences, Amersham, UK). Nonspecific sites were blocked by incubation of the membrane in blocking buffer [5% nonfat dry milk in T-TBS (TBS containing 0.05% Tween 20)] at room temperature for 1 h. Then the membranes were incubated with the indicated primary antibody [endothelial nitric oxide synthase (eNOS) (1:1000, Cell signaling), NOX1 (1:4000, Sigma), NOX2 (1:4000, Sigma), NOX4 (1:4000, Abcam), CD31 (1:3000, Abcam), von Willebrand factor

Endothelial progenitor cells and SNAP for limb ischemia

(vWF) (1:3000, Abcam), cleaved caspase 3 (1:1000, Cell Signaling), cleaved Poly (ADP-ribose) polymerase (PARP) (1:1000, Cell Signaling), cyto-cytochrome C (1:10000, BD), phosphorylated (p)-DRP1 (1:1000, Cell signaling), total DRP1 (1:1000, Cell Signaling), stromal-cell derived factor (SDF)-1 α (1:1000, Cell Signaling), vascular endothelial growth factor (VEGF) (1:4000, Abcam), p-Smad3 (1:1000, Cell Signaling), total Samd3 (1:1000, Cell Signaling), tissue growth factor beta (TGF- β) (1:3000, Abcam), matrix metalloproteinase (MMP)-9 (1:4000, Abcam), nuclear factor (NF)- κ B (1:1000, Cell Signaling), tumor necrosis factor (TNF)- α (1:1000, Cell Signaling), interleukin (IL)-1 β (1:1000, Cell Signaling) and actin (1:10000, Chemicon, Billerica, MA, USA)] for 1 h at room temperature. Horseradish peroxidase-conjugated anti-rabbit immunoglobulin IgG (1:2000, Cell Signaling) was used as a secondary antibody for one-hour incubation at room temperature. After being washed, the immunoreactive membranes were visualized by enhanced chemiluminescence (ECL; Amersham Biosciences) and were exposed to Biomax L film (Kodak, Rochester, NY, USA). For the purpose of quantification, ECL signals were digitized using Labwork software (UVP, Waltham, MA, USA).

We used 6 animals per group for each experiment, indicating 6 sets of samples were prepared for each western blot. In each set of samples, we utilized the antibody against actin for a loading control and normalization. Therefore, if the presented pictures of western blotting against different proteins were derived from the same set of samples, the images of actin for normalization should be the same ones.

Small vessel density in limb ischemic area

Immunohistochemical (IHC) staining of blood vessels was performed with α -smooth muscle actin (SMA) (1:700, Sigma-Aldrich, Massachusetts, USA) as primary antibody at room temperature for 1 h, followed by washing with PBS three times. Ten minutes after the addition of the anti-mouse-HRP conjugated secondary antibody, the tissue sections will be washed with PBS three times. Then 3,3' diaminobenzidine (DAB) (0.7 gm/tablet) (Sigma) was added, followed by washing with PBS three times after one minute. Finally, hematoxylin was added as

a counter-stain for nuclei, followed by washing twice with PBS after one minute. Three sections of quadriceps were analyzed in each animal. For quantification, three randomly selected HPFs ($\times 100$) were analyzed in each section. The mean number per HPF for each animal was then determined by summation of all numbers divided by 9.

Statistical analysis

Quantitative data were expressed as mean \pm SD. Statistical analysis was adequately performed by an analysis of variance (ANOVA) followed by Bonferroni multiple comparison post hoc test. Statistical analysis was performed using SAS statistical software for Windows version 8.2 (SAS Institute, Cary, NC, USA). A *p* value of less than 0.05 was considered significant.

Results

Cell viability, reactive oxygen species, cellular apoptosis, integrity of endothelial function, mitochondrial level of Mel, and protein level of oxidative stress (Figures 1 and 2)

The MTT assay demonstrated that the cell viability at the time points of 24, 48, and 72 h was significantly lower in A2 (i.e., EPCs + Mena) as compared to A1 (EPCs). This was significantly reversed in A3 (EPCs + Mena + Mel) and more significantly reversed in A4 (EPC^{SW-Mel} + Mena) (**Figure 1**). Additionally, flow cytometric analysis showed that the early (AN-V⁺/PI⁻) and late (AN-V⁺/PI⁺) cellular apoptosis exhibited an identical pattern of ROS among the groups (**Figure 1**) in A1, highest in A2 and significantly higher in A3 than in A4 (**Figure 1**). Furthermore, flow cytometric analysis demonstrated that the total intracellular and mitochondrial ROS were lowest.

The protein expression of phosphorylated endothelial nitric oxide synthase (p-eNOS), an indicator of endothelial functional integrity and capacity of NO production, was highest in A1, lowest in A2, and significantly higher in A4 than in A3. On the one hand, the protein expression of NOX-1, NOX-2 and oxidized protein, three indices of oxidative stress, were highest in A2, lowest in A1 and significantly higher in A3 than in A4 (**Figure 2**). On the other hand, the IF microscopic finding showed that expression of

Endothelial progenitor cells and SNAP for limb ischemia

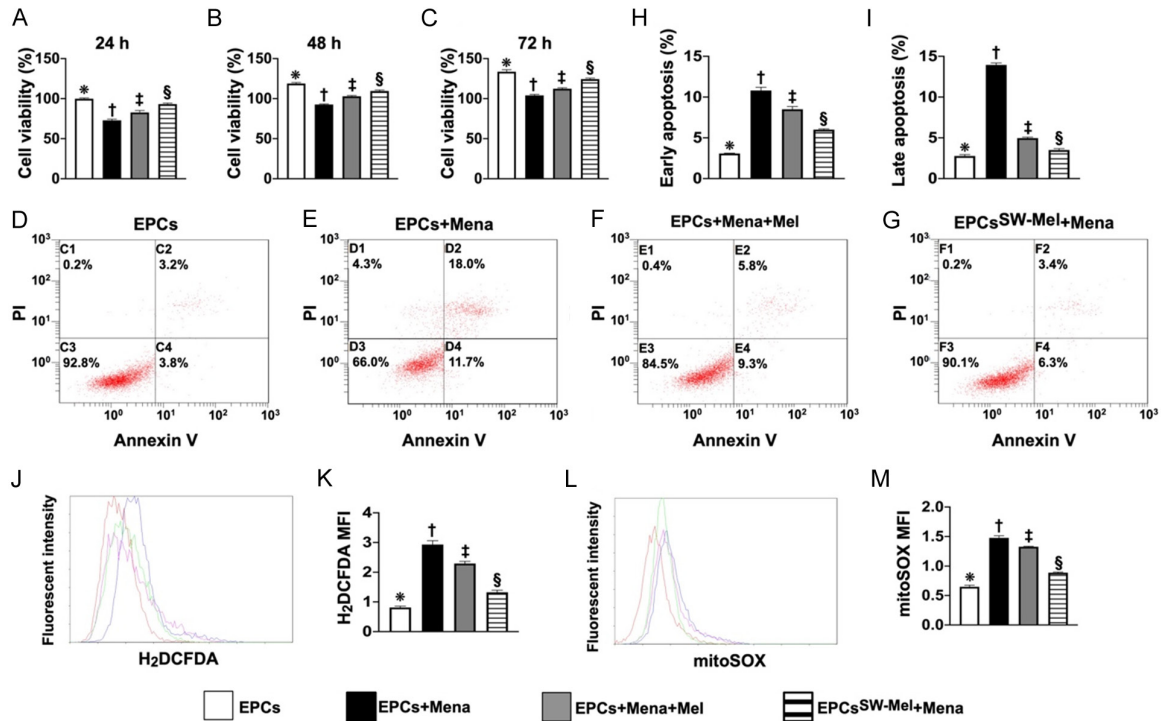


Figure 1. Cell viability, cellular apoptosis, and reactive oxygen species (ROS). A. MTT assay for determining the cell viability at time point of 24 h, * vs. other groups with different symbols (†, ‡, §), $P < 0.0001$. B. MTT assay for determining the cell viability at the time point of 48 h, * vs. other groups with different symbols (†, ‡, §), $P < 0.0001$. C. MTT assay for determining the cell viability at the time point of 72 h, * vs. other groups with different symbols (†, ‡, §), $P < 0.0001$. D-G. Flow cytometric analysis for identification of cell apoptosis. H. Flow cytometric analysis for determining the number of early cellular apoptosis cells (AN-V⁺/PI⁺), * vs. other groups with different symbols (†, ‡, §), $P < 0.0001$. I. Flow cytometric analysis for determining the number of late cellular (AN-V⁺/PI⁺), * vs. other groups with different symbols (†, ‡, §), $P < 0.0001$. J. Flow cytometric analysis for identification of total intracellular ROS. K. Flow cytometric analysis for assessment of mean fluorescent intensity of total intracellular ROS (i.e., stained carboxy-H₂DCFDA dye), * vs. other groups with different symbols (†, ‡, §), $P < 0.0001$. L. Flow cytometric analysis for identification of mitochondrial ROS. M. Flow cytometric analysis for assessment of mean fluorescent intensity of mitochondrial ROS, * vs. other groups with different symbols (†, ‡, §), $P < 0.0001$. All statistical analyses were performed by one-way ANOVA, followed by Bonferroni multiple comparison post hoc test ($n = 4$ for each group). Symbols (*, †, ‡) indicate significance for each other (at 0.05 level). EPCs = endothelial progenitor cells; Mel = melatonin; Mena = menadione. A1 = EPCs only; A2 = EPCs + Mena; A3 = EPCs + Mena + Mel; A4 = EPC^{SW-Mel} + Mena.

number of NO⁺ cells displayed an identical pattern of p-eNOS among the groups (**Figure 2**).

The Mel in mitochondria of the EPCs was conducted. The result showed that mitochondrial concentration of Mel was significantly higher in EPC^{SW-Mel} than in EPC + Mel and the control, and significantly higher in EPC + Mel than in the control (**Figure 2**), implying that ECSW treatment could facilitate Mel entry into the EPC mitochondria.

We tentatively concluded that the above-mentioned findings (i.e., **Figures 1** and **2**) showed that ECSW-supported Mel protected EPCs against Mena damage.

SNAP treatment upregulated NO production and angiogenesis and generation of soluble angiogenesis factors (Figure 3)

The results of Matrigel assay demonstrated that the angiogenesis capacity was significantly higher in B2 (i.e., EPCs + snap) than in B1 (EPCs). Additionally, the IF microscopic findings identified that the number of positively stained NO cells and (by western blot analysis) the protein expressions of eNOS, CD31, and vWF, three indicators of integrity of endothelial function, exhibited an identical pattern between groups B1 and B2. Our findings suggest that SNAP could be a NO donor/stimulator for facilitating the integrity of endothelial cell function.

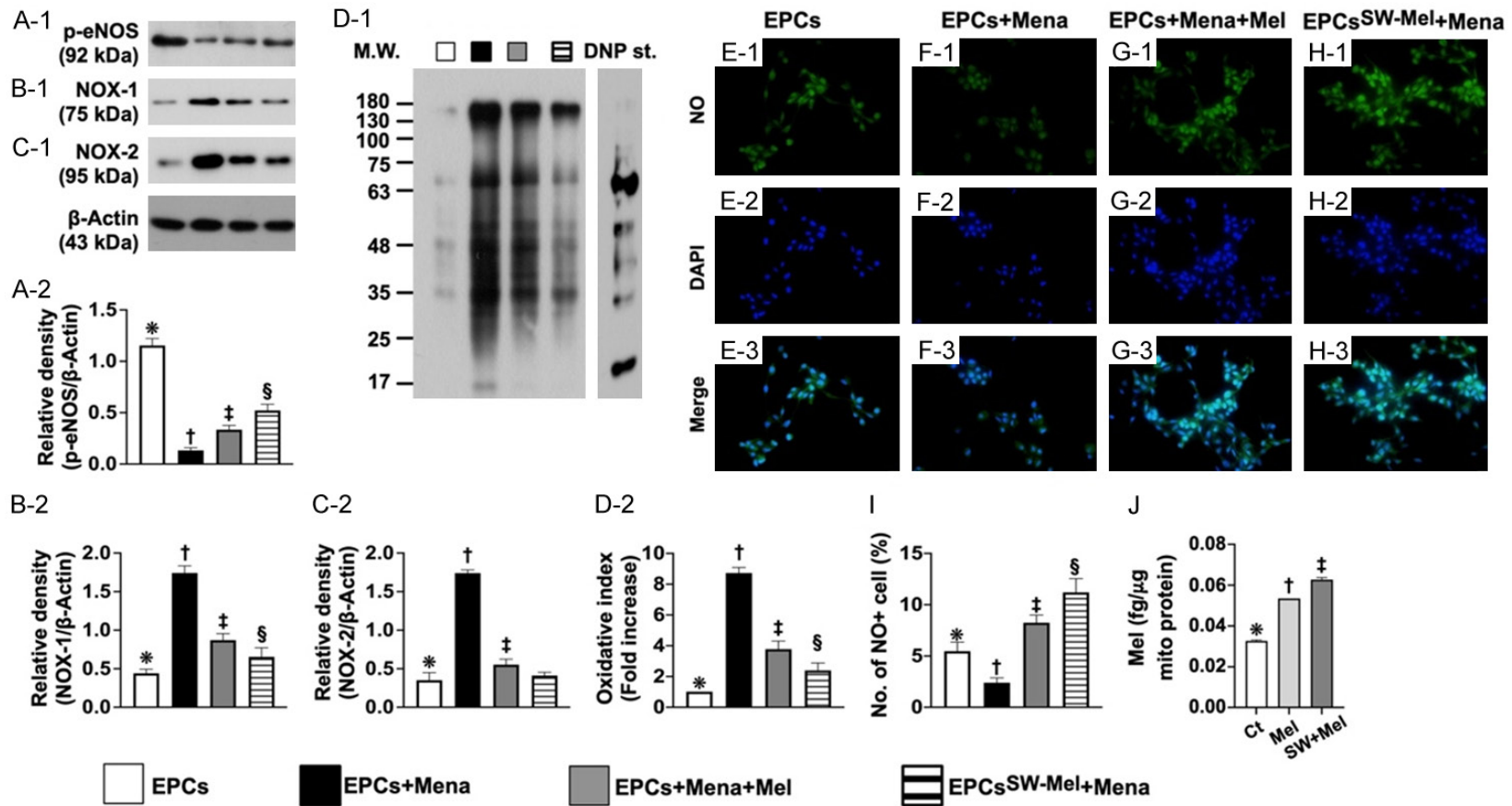


Figure 2. Integrity of endothelial function, protein level of oxidative stress, and mitochondrial concentration of Mel in EPCs. (A) Protein expression of phosphorylated endothelial nitric oxide synthase (p-eNOS), * vs. other groups with different symbols (†, ‡, §), $P < 0.0001$. (B) Protein expression of NOX-1, * vs. other groups with different symbols (†, ‡, §), $P < 0.0001$. (C) Protein expression of NOX-2, * vs. other groups with different symbols (†, ‡, §), $P < 0.0001$. (D) Expression of oxidized protein, * vs. other groups with different symbols (†, ‡), $P < 0.001$ (Note: the left and right lanes shown on the upper panel represent protein molecular weight marker and control oxidized molecular protein standard, respectively). M.W. = molecular weight; DNP = 1-3 dinitrophenylhydrazine. (E-H) Immunofluorescent (IF) microscopic finding (400 \times) for identification of positively stained nitric oxide (NO) in EPCs (green color). Blue color indicated DAPI stain (i.e., E-2-H-2) for identification of nuclei. Light green color indicated merged picture (E-3-H-3). (I) Analytical result of number of NO+ cells, * vs. other groups with different symbols (†, ‡, §), $P < 0.0001$. Scale bar in right lower corner represents 20 μ m. (J) Mitochondrial concentration of Mel in EPCs, * vs. other groups with different symbols (†, ‡), $P < 0.0001$. All statistical analyses were performed by one-way ANOVA, followed by Bonferroni multiple comparison post hoc test ($n = 4$ for each group). Symbols (*, †, ‡) indicate significance for each other (at 0.05 level). EPCs = endothelial progenitor cells; Mel = melatonin; Mena = menadione. A1 = EPCs only; A2 = EPCs + Mena; A3 = EPCs + Mena + Mel; A4 = EPC^{SW-Mel} + Mena.

Endothelial progenitor cells and SNAP for limb ischemia

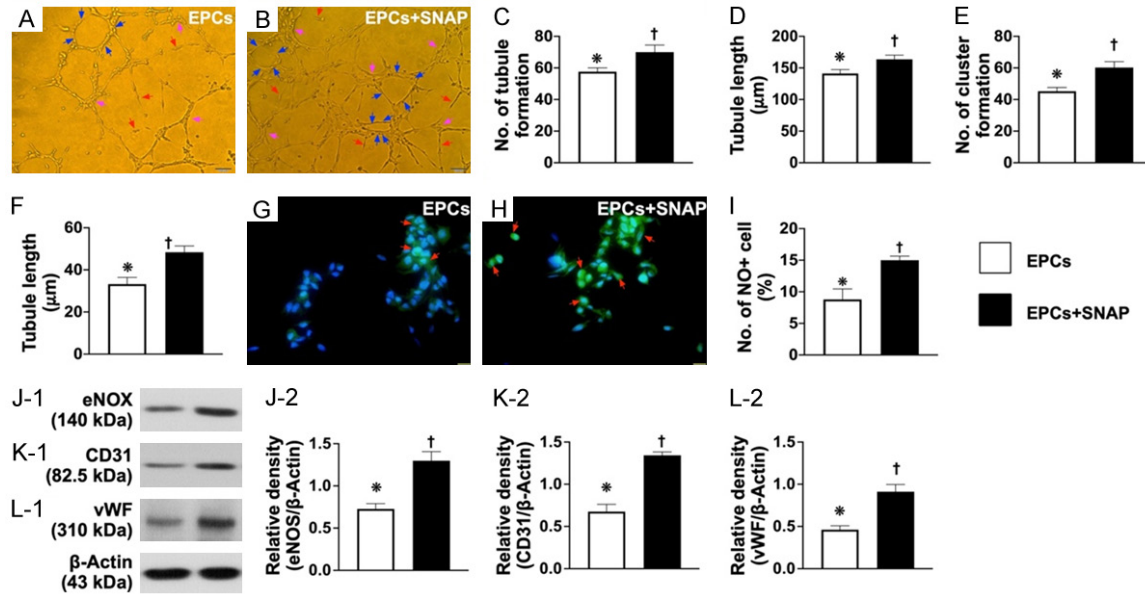


Figure 3. SNAP treatment upregulated angiogenesis, NO production, and generation of soluble angiogenesis factors. A and B. Angiogenesis feature by Matrigel assay showed that the angiogenesis capacity was significantly increased in EPCs treated by SNAP compared to EPCs only (i.e., control group). C. Number of tubules formed (red arrows), * vs. †, $P < 0.0001$. D. Tubule length, * vs. †, $P < 0.0001$. E. Number of clusters formed (pink arrows), * vs. †, $P < 0.0001$. F. Number of networks formation (blue color), * vs. †, $P < 0.0001$. G and H. Immunofluorescent microscopic findings (400 ×) for identification of positively stained nitric oxide (NO) cells (green color) (red arrows). Scale bar in right lower corner represents 20 μm. I. Analytical result of number of NO+ cells, * vs. †, $P < 0.0001$. J. Protein expression of endothelial nitric oxide synthase (eNOS), * vs. †, $P < 0.0001$. K. Protein expression of CD31, * vs. †, $P < 0.0001$. L. Protein expression of von Willebrand factor (vWF), * vs. †, $P < 0.0001$. $n = 4$ for all groups. SNAP = S-nitroso-N-acetyl-DL-penicillamine; EPCs = endothelial progenitor cells; B1 = EPCs only; B2 = EPCs + SNAP.

Ex vivo carotid artery angiogenesis (Figure 4)

The ex vivo carotid artery angiogenesis was determined by microscope. Results showed that the angiogenesis capacity of the carotid ring was lowest in group C, highest in group B, and significantly lower in group D than in group A, suggesting SNAP played a crucial role in enhancing ex vivo carotid artery angiogenesis.

Carotid artery relaxation and NO release (Figure 5)

Baseline NO release from the LCCA was significantly higher in B than in other groups, significantly higher in A than in C and D, and significantly higher in D than in C.

Additionally, to elucidate the impact of Mena and SNAP on regulating vessel relaxation and contraction, the LCCA was cut into pieces and mounted on the machine system. As expected, vasoconstriction exhibited an opposite pattern, whereas vasorelaxation exhibited an identical pattern of NO release among the groups.

Ischemic to normal blood flow (INBF) ratio analyzed by laser Doppler scan by days 1, 7, and 14 after conducting left CLI procedure (Figure 6)

By day 0 prior to CLI procedure, the INBF did not differ among the four groups. By day 1 after CLI induction, laser Doppler examination demonstrated a significantly higher INBF ratio in group 1 (SC) than in group 2 (CLI), group 3 (CLI + SNAP), group 4 (CLI + EPC^{SW-Mel}), or group 5 (CLI + EPC^{SW-Mel} + SNAP), but there was no significant difference among the latter four groups. However, by days 7 and 14 after induction of CLI, the ratio of INBF was highest in group 1, lowest in group 2, and significantly and progressively increased from groups 3 to 5.

Protein expressions of oxidative stress, apoptosis, and mitochondrial damage in CLI by day 14 after CLI induction (Figure 7)

Western blot analysis demonstrated that the protein expressions of NOX-1, NOX-4, and oxidized protein, three indices of oxidative stress, protein expressions of cleaved caspase 3 and

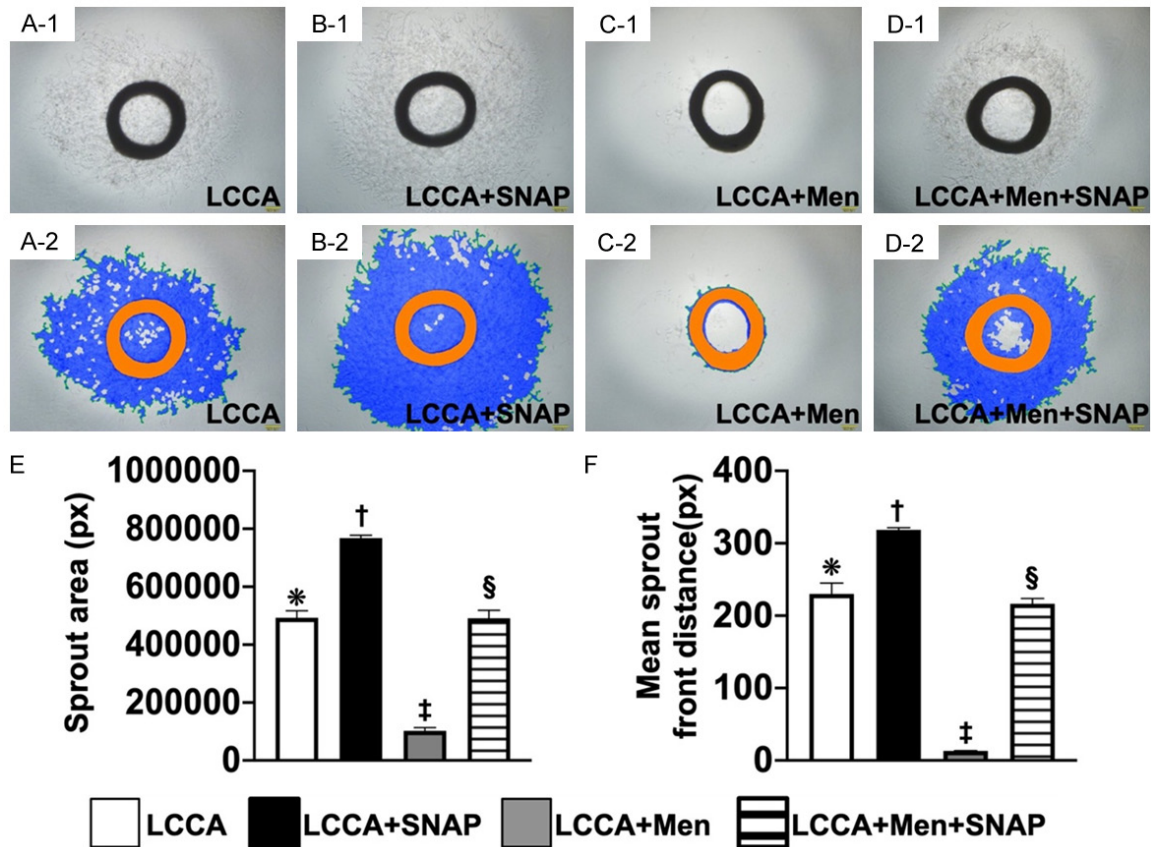


Figure 4. Ex vivo culture of carotid artery angiogenesis. (A-D) Light microscopic findings (i.e., photographic images) (100 ×) of carotid ring culturing in groups A (i.e., SC) (A-1, A-2), B (B-1, B-2), C (C-1, C-2), and D (D-1, D-2), respectively. Scale bar in right lower corner represents 100 μm. (E) Analytical results of sprout area, * vs. other groups with different symbols (†, ‡, §), $P < 0.0001$. (F) Analytic result of mean sprout front distance, * vs. other groups with different symbols (†, ‡, §), $P < 0.0001$. All statistical analyses were performed by one-way ANOVA, followed by Bonferroni multiple comparison post-hoc test ($n = 6$ for each group). Symbols (*, †, ‡, §) indicate significance at 0.05 level. LCCA = left common carotid artery; SNAP = S-nitroso-N-acetyl-DL-penicillamine; Men = menadione; group A (LCCA only), group B (LCCA + SNAP), group C (LCCA + Men) and group D (LCCA + Men + SNAP).

cleaved PARP, two indicators of apoptosis, and protein expressions of cytosolic cytochrome C and phosphorylated (p)-DRP-1, two mitochondrial-damaged markers, were highest in group 2, lowest in group 1, and significantly and progressively reduced from groups 3 to 5.

Protein expressions of endothelial cell surface markers, small vessel density, and angiogenesis biomarkers in CLI by day 14 after CLI induction (Figure 8)

The protein expressions of CD31, vWF, and eNOS, three indicators of endothelial cell surface markers, were highest in group 1, lowest in group 2, and progressively increased from groups 3 to 5. Additionally, the IHC microscopic finding revealed that the number of small ves-

sels (i.e., defined as diameter ≤ 25.0 μM) exhibited an identical pattern of DC31 among the five groups.

The protein expressions of SDF-1α and VEGF, two indicators of angiogenesis factors, were progressively increased from groups 1 to 5, indicating an intrinsic response to CLI stimulation and significantly enhanced by the different treatment strategies.

Protein expressions of fibrotic and inflammatory biomarkers in CLI by day 14 after CLI induction (Figure 9)

The protein expressions of Smad3 and TGF-β, two indicators of fibrosis, and the protein expressions of MMP-9, NF-κB, TNF-α, IL-1β,

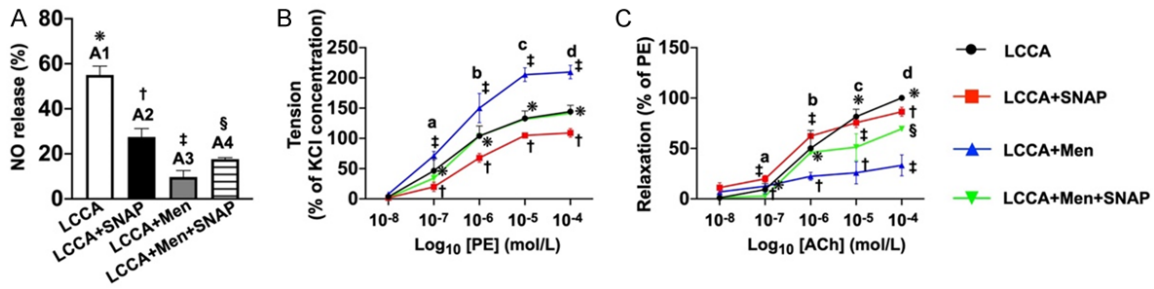


Figure 5. Ex vivo carotid artery relaxation and NO release. A. Schematic illustration of NO release from endothelial cells of LCCA from sham-control group (A1) indicating the native endothelial cells (ECs) of LCCA without any pre-treatment. On the other hand, A2 to A4 groups were pretreated by L-NAME (100 μM) for 30 minutes. NO release (%) was significantly attenuated in A2 (i.e., LCCA + SNAP) as compared to the A1. It was further significantly attenuated in A3 (LCCA + Men). This was partially but significantly reversed in A4 (LCCA + Men + SNAP), implying that SNAP plays a crucial role in stimulating the ECs to release NO. Analytical result of NO release (%) among the four groups, * vs. other groups with different symbols (†, ‡, §), P<0.0001. B. Phenylephrine (PE) concentration-response curves (i.e., tension) in LCCA. The cumulative concentration-response curve of LCCA constriction normalized to 90 mM potassium chloride (KCl)-induced contraction. The 4 curves, indicating the 4 individual groups, illustrated a stepwise-increased concentration of PE-induced increase in vasoconstriction. This was significantly and progressively increased in group C compared to other groups. Analytical result of vasoconstriction (%), * vs. other groups with different symbols (†, ‡, §) at point a, P<0.0001. Additionally, analytical result of vasoconstriction (%), * vs. other groups with different symbols (†, ‡) at points b, c and d [i.e., among the groups in different points (i.e., b, c, d) of concentrations], P<0.0001. C. The LCCA dilation response to Acetylcholinesterase (ACh) (1.0 × 10⁻⁸ to 3.0 × 10⁻³ M) treatment is presented with respect to the percentage of the contractile response that was induced by phenylephrine (PE, 10⁻⁶ M). Additionally, ACh-induced vasorelaxation was significantly reduced in group B versus other groups. Analytical result of vasorelaxation (%), * vs. other groups with different symbols (†, ‡), P<0.0001, i.e., * vs. other groups with different symbols (†, ‡) at points a, b and c [i.e., among the four groups in different points (i.e., a, b, c) of concentration] and * vs. other groups with different symbols (†, ‡, §) at point d. All statistical analyses were performed by one-way ANOVA, followed by Bonferroni multiple comparison post-hoc test (n = 6 for each group). Symbols (*, †, ‡, §) indicate significance (at 0.05 level). LCCA = left common carotid artery; SNAP = S-nitroso-N-acetyl-DL-penicillamine; Men = menadione; NO = nitric oxide; group A (LCCA only), group B (LCCA + SNAP), group C (LCCA + Men) and group D (LCCA + Men + SNAP).

four indicators of inflammation, were highest in group 1, lowest in group 2, and significantly progressively reduced from groups 3 to 5.

Discussion

This study investigated the therapeutic impact of ECSW-facilitated Mel delivered into EPCs and NO donor. There were several striking implications. First, the *in vitro* study demonstrated that as compared to the control (i.e., EPCs only), EPC^{SW-Mel} had a greater ability to resist oxidative stress and improved the cell viability and NO production. Second, *in vitro*, *ex vivo* and *in vivo* studies showed that SNAP treatment offered a great benefit on generation of soluble angiogenesis factors, NO production, angiogenesis, and vasorelaxation. Third, combined EPC^{SW-Mel} and SNAP treatment was more effective than merely one for restoring the blood flow in CLI and rescuing the critical limb ischemia in rats.

Currently, the treatment of CLTI/CLI is still a formidable challenge not only because of the high

frequency of requirement for amputation and the low frequency of the amputation-free rate [14], but also the low overall survival rate [3, 8, 9, 11, 15]. This shows that the treatment of these disease entities is still an unmet need, and therefore, an innovative treatment must be urgently found. The most important finding of the present study was that as compared to CLI only, the INBF ratio was significantly increased in EPC, SNAP, or EPC^{SW-Mel} treatment and more significantly increased by combined EPC^{SW-Mel} and SNAP treatment. Our findings highlight that a combination regimen (i.e., EPC^{SW-Mel} + SNAP) could be a last resort for those of CLTI/CLI patients who are refractory to conventional therapy.

An mechanistic explanation is needed for why the combined regimen was superior to either one treatment. It is well-known that inflammation and oxidative stress always are elicited in ischemic tissues/organs [5, 8, 9, 18-20], resulting in damaging and shortening the survival rate of EPCs in the ischemic zone [16, 17].

Endothelial progenitor cells and SNAP for limb ischemia

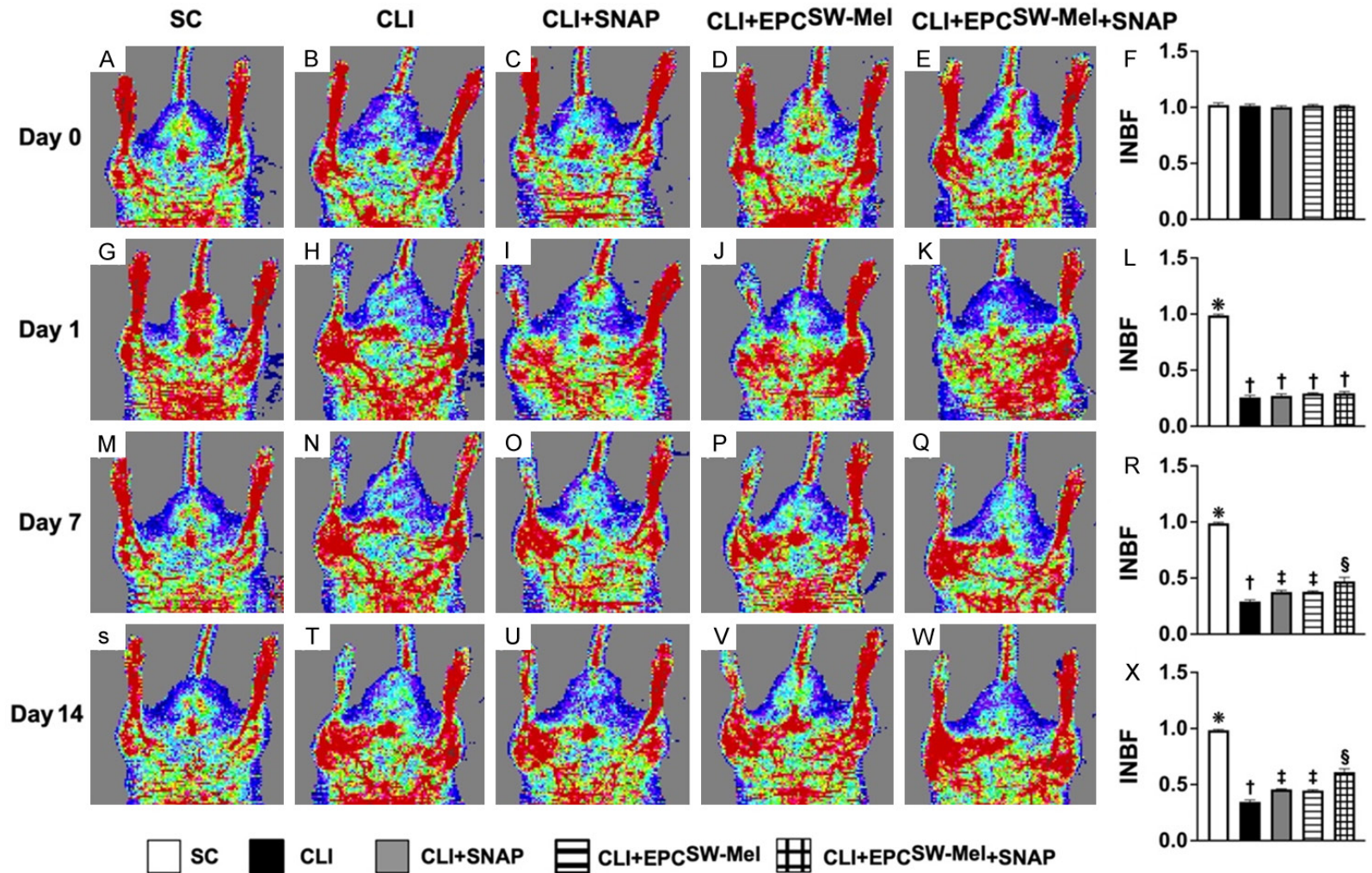


Figure 6. Ischemic to normal blood flow (INBF) ratio analyzed by laser Doppler scan by days 0, 1, 7, and 14 after conducting left CLI induction. A-E. Laser Doppler finding of ratio of left limb (ischemia) to right limb (normal) blood flow (i.e., INBF) at day 0 prior to CLI procedure among the five groups. F. Analytical result of ratio of INBF, $P > 0.5$. G-K. Laser Doppler finding of INBF at day 1 after CLI induction among the five groups. L. Analytical result of ratio of INBF, * vs. †, $P < 0.0001$, $P < 0.0001$. M-Q. Laser Doppler finding of ratio of INBF at day 7 after CLI induction among the five groups. R. Analytical result of ratio of INBF, * vs. other groups with different symbols (†, ‡, §), $P < 0.0001$. S-W. Laser Doppler finding of ratio of INBF at day 14 after CLI procedure among the five groups. X. Analytical result of ratio of INBF, * vs. other groups with different symbols (†, ‡, §), $P < 0.0001$. All statistical analyses were performed by one-way ANOVA, followed by Bonferroni multiple comparison post hoc test ($n = 10$ for each group). Symbols (*, †, ‡, §) indicate significance (at 0.05 level). CLI = critical limb ischemia; SNAP = S-nitroso-N-acetyl-DL-penicillamine; SC = sham-operated control; EPC^{SW-Mel} = extracorporeal shock wave (ECSW) facilitated melatonin (Mel) delivery into autologous endothelial progenitor cells (EPCs); group 1 = SC; group 2 = CLI; group 3 = CLI + SNAP; group 4 = CLI + EPC^{SW-Mel}; group 5 = CLI + EPC^{SW-Mel} + SNAP.

Endothelial progenitor cells and SNAP for limb ischemia

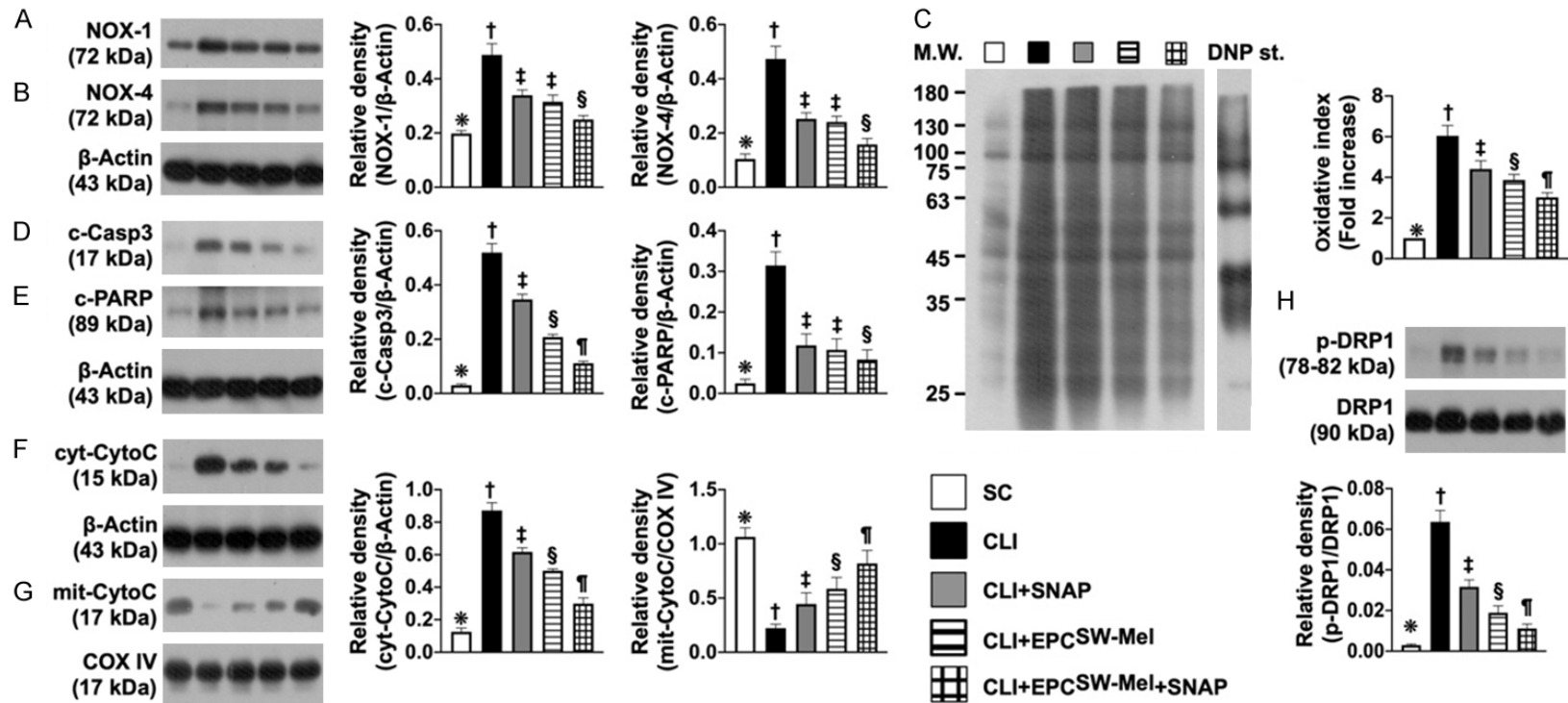


Figure 7. Protein expressions of oxidative stress, apoptosis, and mitochondrial damage in CLI by day 14 after CLI induction. A. Protein expression of NOX-1, * vs. other groups with different symbols (†, ‡, §), $P < 0.0001$. B. Protein expression of NOX-4, * vs. other groups with different symbols (†, ‡, §), $P < 0.0001$. C. The oxidized protein expression, * vs. other groups with different symbols (†, ‡, §, ¶), $P < 0.0001$ (Note: the left and right lanes shown on the upper panel represent protein molecular weight marker and control oxidized molecular protein standard, respectively). M.W. = molecular weight; DNP = 1-3 dinitrophenylhydrazone. D. Protein expression of cleaved caspase 3 (c-Casp3), * vs. other groups with different symbols (†, ‡, §, ¶), $P < 0.0001$. E. Protein expression of cleaved poly (ADP-ribose) polymerase (c-PARP), * vs. other groups with different symbols (†, ‡, §), $P < 0.0001$. F. Protein expression of cytosolic cytochrome C (cyt-CytoC), * vs. other groups with different symbols (†, ‡, §, ¶), $P < 0.0001$. G. Protein expression of mitochondrial cytochrome C (mit-CytoC), * vs. other groups with different symbols (†, ‡, §, ¶), $P < 0.0001$. H. Protein expression of phosphorylated dynamin-1-like protein (p)-DRP-1, * vs. other groups with different symbols (†, ‡, §, ¶), $P < 0.0001$. All statistical analyses were performed by one-way ANOVA, followed by Bonferroni multiple comparison post hoc test ($n = 6$ for each group). Symbols (*, †, ‡, §, ¶) indicate significance (at 0.05 level). SC = sham-operated control; EPC^{SW-Mel} = extracorporeal shock wave (ECSW) facilitated melatonin (Mel) delivery into autologous endothelial progenitor cells (EPCs); CLI = critical limb ischemia; SNAP = S-nitroso-N-acetyl-DL-penicillamine; group 1 = SC; group 2 = CLI; group 3 = CLI + SNAP; group 4 = CLI + EPC^{SW-Mel}; group 5 = CLI + EPC^{SW-Mel} + SNAP.

Endothelial progenitor cells and SNAP for limb ischemia

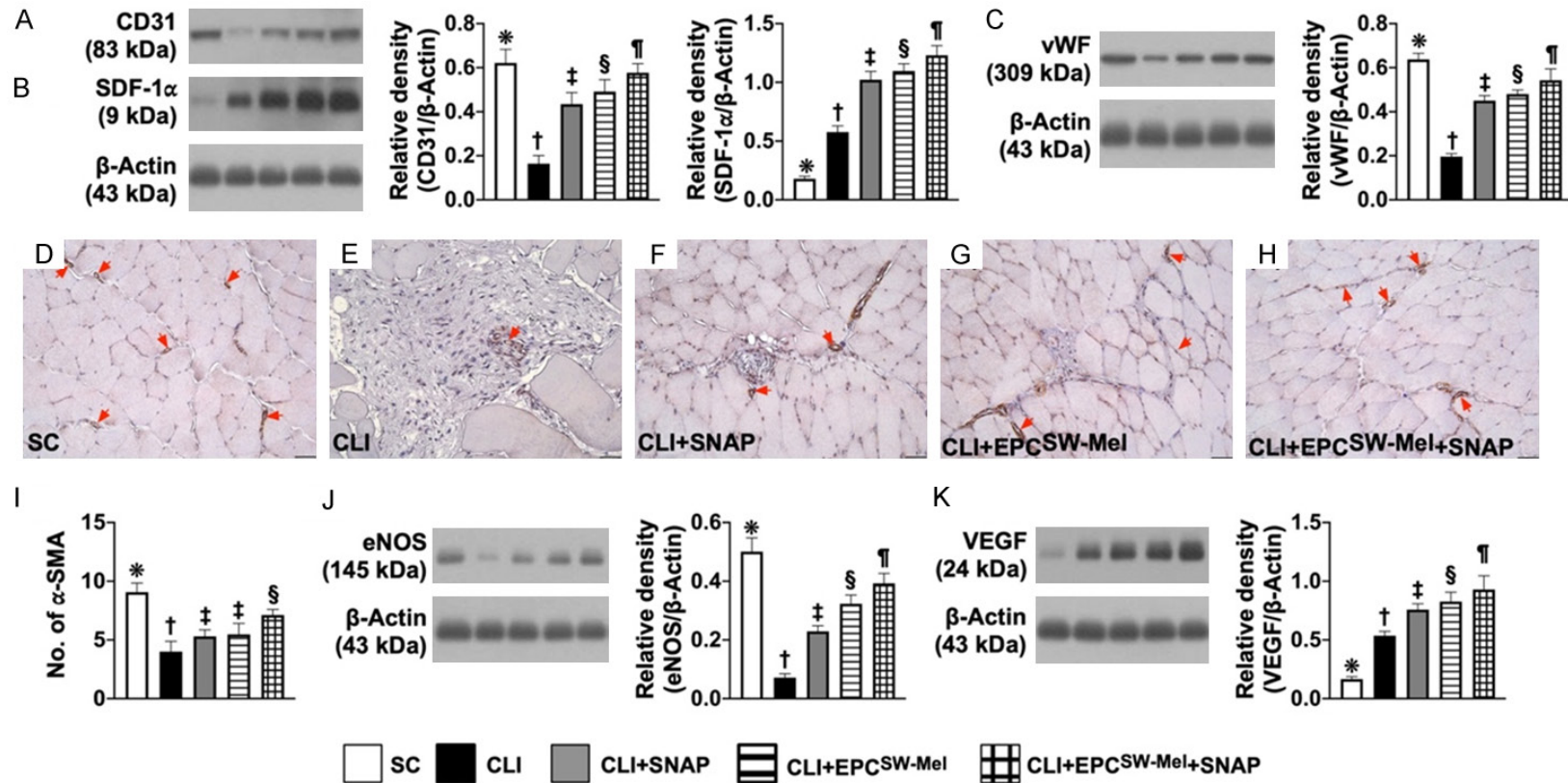


Figure 8. Protein expressions of endothelial cell surface markers, small vessel density, and angiogenesis biomarkers in CLI by day 14 after CLI induction. A. Protein expression of CD31, * vs. other groups with different symbols (†, ‡, §, ¶), $P < 0.0001$. B. Protein expression of stromal-cell derived factor 1 alpha (SDF-1 α), * vs. other groups with different symbols (†, ‡, §, ¶), $P < 0.0001$. C. Protein expression of von Willebrand factor (vWF), * vs. other groups with different symbols (†, ‡, §, ¶), $P < 0.0001$. D-H. Microscopic findings (100 \times) for identification of positively-stained alpha smooth muscle actin (α -SMA) small vessels (gray color, red arrows). I. Number of small vessels (i.e., defined as diameter ≤ 25.0 μ m), * vs. other groups with different symbols (†, ‡, §), $P < 0.0001$. J. Protein expression of endothelial nitric oxide synthase (eNOS), * vs. other groups with different symbols (†, ‡, §, ¶), $P < 0.0001$. K. Protein expression of vascular endothelial growth factor (VEGF), * vs. other groups with different symbols (†, ‡, §, ¶), $P < 0.0001$. All statistical analyses were performed by one-way ANOVA, followed by Bonferroni multiple comparison post-hoc test ($n = 6$ for each group). Symbols (*, †, ‡, §, ¶) indicate significance (at 0.05 level). SC = sham-operated control; EPC^{SW-Mel} = extracorporeal shock wave (ECSW) facilitated melatonin (Mel) delivery into autologous endothelial progenitor cells (EPCs); SNAP = S-nitroso-N-acetyl-DL-penicillamine; group 1 = SC; group 2 = CLI; group 3 = CLI + SNAP; group 4 = CLI + EPC^{SW-Mel}; group 5 = CLI + EPC^{SW-Mel} + SNAP.

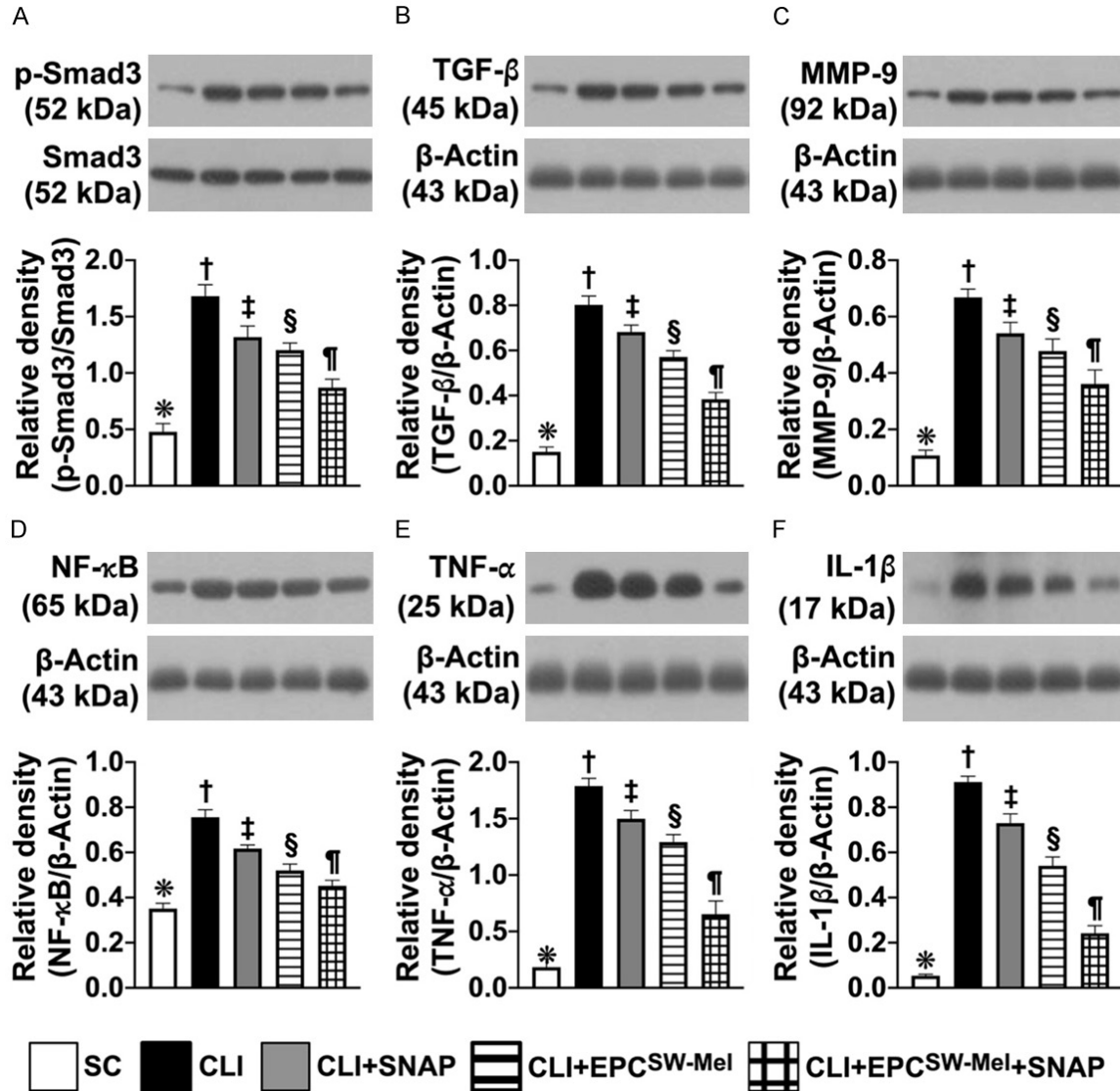


Figure 9. Protein expressions of fibrotic and inflammatory biomarkers in CLI by day 14 after CLI induction. A. Protein expression of phosphorylated (p)-Smad3, * vs. other groups with different symbols (†, ‡, §, ¶), $P < 0.0001$. B. Protein expression of transforming growth factor beta (TGF- β), * vs. other groups with different symbols (†, ‡, §, ¶), $P < 0.0001$. C. Protein expression of matrix metalloproteinase (MMP)-9, * vs. other groups with different symbols (†, ‡, §, ¶), $P < 0.0001$. D. Protein expression of phosphorylated (p) nuclear factor (NF)- κ B, * vs. other groups with different symbols (†, ‡, §, ¶), $P < 0.0001$. E. Protein expression of tumor necrosis factor (TNF)- α , * vs. other groups with different symbols (†, ‡, §, ¶), $P < 0.0001$. F. Protein expression of interleukin (IL)-1 β , * vs. other groups with different symbols (†, ‡, §, ¶), $P < 0.0001$. All statistical analyses were performed by one-way ANOVA, followed by Bonferroni multiple comparison post-hoc test ($n = 6$ for each group). Symbols (*, †, ‡, §, ¶) indicate significance (at 0.05 level). SC = sham-operated control; EPC^{SW-Mel} = extracorporeal shock wave (ECSW) facilitated melatonin (Mel) delivery into autologous endothelial progenitor cells (EPCs); CLI = critical limb ischemia; SNAP = S-nitroso-N-acetyl-DL-penicillamine; group 1 = SC; group 2 = CLI; group 3 = CLI + SNAP; group 4 = CLI + EPC^{SW-Mel}; group 5 = CLI + EPC^{SW-Mel} + SNAP.

Several studies have already shown that Mel has a strong capacity of suppressing inflammation and oxidative stress as well as protecting the integrity of EPCs [28-33]. Interestingly, our *in vitro* study discovered that ECSW treatment can enhance Mel delivery into the EPCs, result-

ing in inhibiting oxidative stress production. These aforementioned reports and the result of our *in vitro* study put together may, at least in part, explain why EPC^{SW-Mel} was superior to EPCs only for restoring the blood flow in the CLI area and salvaging the ischemic limb in rats.

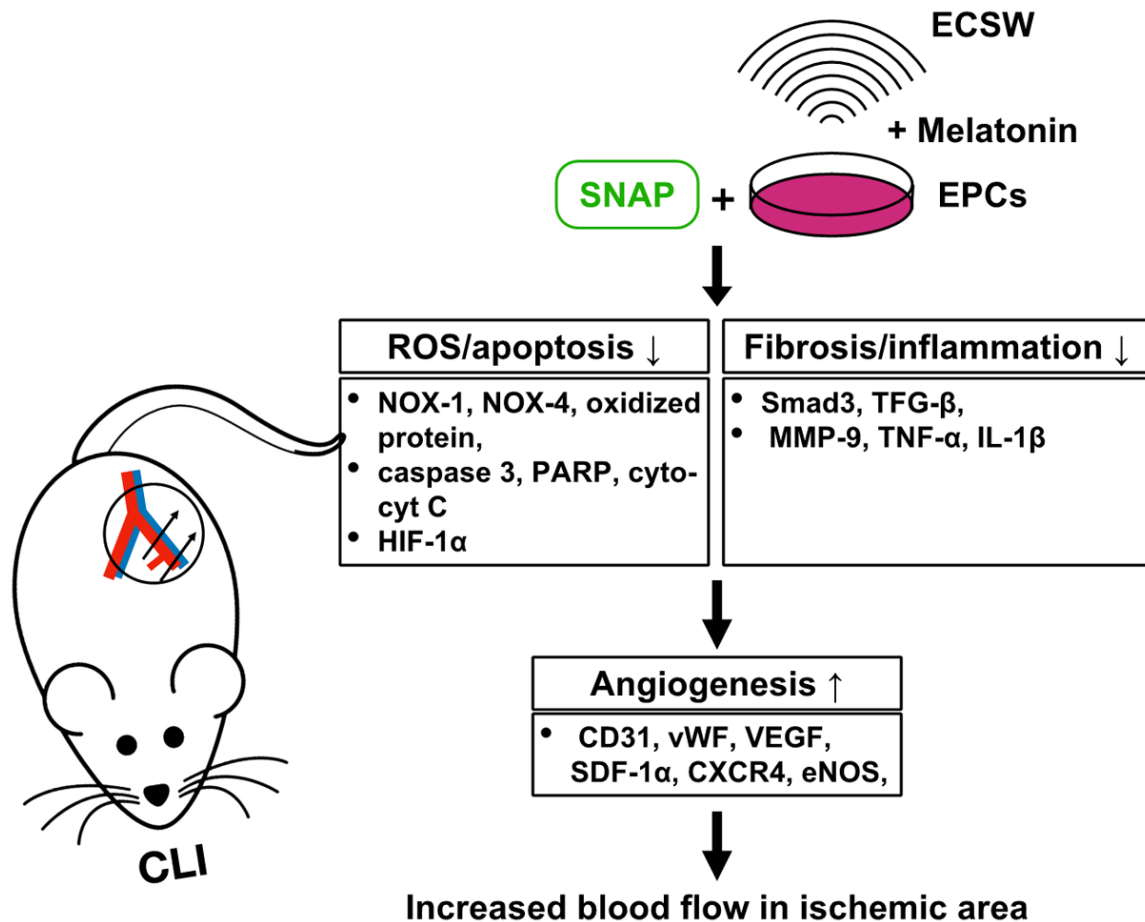


Figure 10. Schematic figure of the underlying mechanism of EPC^{SW-Mel} and SNAP treatment on restoring the blood flow to the CLI area and rescuing the critical limb. CLI = critical limb ischemia; SNAP = S-nitroso-N-acetyl-DL-penicillamine; EPCs = endothelial progenitor cells; ECSW = extracorporeal shock wave; ROS = reactive oxygen species; cyt-cyt C = cytosolic cytochrome C; SDF-1 α = stromal cell-derived factor 1 alpha.

SNAP has been shown to serve as a NO donor [36-39]. Additionally, NO, which is an indicator of endothelial cell integrity, plays a crucial role in vessel dilatation and the generation of angiogenesis factors. An essential finding of our *in vitro* study demonstrated that the angiogenesis of EPCs markedly augmented by SNAP treatment. Another essential finding of our *ex vivo* study demonstrated that angiogenesis of the aortic ring was also markedly augmented by SNAP treatment. Of importance was that SNAP treatment enhanced not only NO release from rat aorta but also rat aortic vasorelaxation. These findings from *in vitro* and *ex vivo* studies supported why the INBF ratio was significantly increased in CLI animals with SNAP compared to those without SNAP treatment. A notable finding was that combined EPC^{SW-Mel} and SNAP treatment was more effective than merely one

treatment, implicating that this combined regimen may offer an additional benefit for restoring the blood flow to the CLI area and rescuing the critical limb in rats.

A link between oxidative stress/inflammation and unfavorable outcomes in setting of ischemic organ damage has been well-recognized [16-20, 28-33]. When we looked at the molecular perturbations in the CLI area, we found that the protein levels of oxidative stress, inflammation, apoptosis, and mitochondrial damage were substantially higher in the CLI area than that of the SC animals. These molecular perturbations in the CLI zone were significantly reversed by EPCs and SNAP treatment, further significantly reversed by EPC^{SW-Mel} treatment, and furthermore significantly reversed by combined EPC^{SW-Mel} and SNAP treatment. In this

way, our findings, in addition to strengthening the findings of previous studies [16-20, 28-33], could partially explain why the untoward outcomes in CLI rodents had various degrees of effective improvement by undergoing different therapeutic regimens.

Study limitations

A first limitation was that the study period was relatively short. Therefore, the long-term effect of combined EPC^{SW-Mel} and SNAP treatment on maintaining adequate blood flow in CLI is still currently unclear. Second, although extensive work was done, the exact underlying mechanism is still unclear but was schematically proposed in **Figure 10** based on the results of our *in vitro*, *ex vivo*, and *in vivo* studies.

In conclusion, the results of the present study demonstrated that combined EPC^{SW-Mel} and SNAP treatment offered great benefits of antioxidant and NO donation to EPCs, resulting in much enhanced angiogenesis, restoring the blood flow in CLI, and therefore salvaging the critical limb in rats.

Disclosure of conflict of interest

None.

Address correspondence to: Dr. Jun Guo, Department of Cardiology, The First Affiliated Hospital, Jinan University, 613 W. Huangpu Avenue, Guangzhou 510630, Guangdong, China. Tel: +86-020-38688963; Fax: +86-030-38688888; E-mail: dr.guojun@163.com; guojun2009@jnu.edu.cn

References

- [1] Criqui MH and Aboyans V. Epidemiology of peripheral artery disease. *Circ Res* 2015; 116: 1509-1526.
- [2] Fowkes FG, Rudan D, Rudan I, Aboyans V, Denenberg JO, McDermott MM, Norman PE, Sampson UK, Williams LJ, Mensah GA and Criqui MH. Comparison of global estimates of prevalence and risk factors for peripheral artery disease in 2000 and 2010: a systematic review and analysis. *Lancet* 2013; 382: 1329-1340.
- [3] Lawall H, Huppert P, Espinola-Klein C and Rumenapf G. The diagnosis and treatment of peripheral arterial vascular disease. *Dtsch Arztebl Int* 2016; 113: 729-736.
- [4] Song P, Rudan D, Zhu Y, Fowkes FJL, Rahimi K, Fowkes FGR and Rudan I. Global, regional, and national prevalence and risk factors for peripheral artery disease in 2015: an updated systematic review and analysis. *Lancet Glob Health* 2019; 7: e1020-e1030.
- [5] Vemulapalli S, Patel MR and Jones WS. Limb ischemia: cardiovascular diagnosis and management from head to toe. *Curr Cardiol Rep* 2015; 17: 611.
- [6] Bauersachs R, Debus S, Nehler M, Huelsebeck M, Balradj J, Bowrin K and Briere JB. A targeted literature review of the disease burden in patients with symptomatic peripheral artery disease. *Angiology* 2020; 71: 303-314.
- [7] Bauersachs R, Zeymer U, Briere JB, Marre C, Bowrin K and Huelsebeck M. Burden of coronary artery disease and peripheral artery disease: a literature review. *Cardiovasc Ther* 2019; 2019: 8295054.
- [8] Lo RC, Bensley RP, Dahlberg SE, Matyal R, Hamdan AD, Wyers M, Chaikof EL and Schermerhorn ML. Presentation, treatment, and outcome differences between men and women undergoing revascularization or amputation for lower extremity peripheral arterial disease. *J Vasc Surg* 2014; 59: 409-418, e403.
- [9] Dayama A, Tsilimparis N, Kolakowski S, Matolo NM and Humphries MD. Clinical outcomes of bypass-first versus endovascular-first strategy in patients with chronic limb-threatening ischemia due to infrageniculate arterial disease. *J Vasc Surg* 2019; 69: 156-163, e151.
- [10] Levin SR, Arinze N and Siracuse JJ. Lower extremity critical limb ischemia: a review of clinical features and management. *Trends Cardiovasc Med* 2020; 30: 125-130.
- [11] Giannopoulos S, Secemsky EA, Mustapha JA, Adams G, Beasley RE, Pliagas G and Armstrong EJ. Three-year outcomes of orbital atherectomy for the endovascular treatment of infringuinal claudication or chronic limb-threatening ischemia. *J Endovasc Ther* 2020; 27: 714-725.
- [12] Jones DW, Dansey K and Hamdan AD. Lower extremity revascularization in end-stage renal disease. *Vasc Endovascular Surg* 2016; 50: 582-585.
- [13] Ouriel K. Peripheral arterial disease. *Lancet* 2001; 358: 1257-1264.
- [14] Conte MS, Bradbury AW, Kolh P, White JV, Dick F, Fitridge R, Mills JL, Ricco JB, Suresh KR, Murad MH, Aboyans V, Aksoy M, Alexandrescu VA, Armstrong D, Azuma N, Belch J, Bergoing M, Bjorck M, Chakfe N, Cheng S, Dawson J, Debus ES, Dueck A, Duval S, Eckstein HH, Ferraresi R, Gambhir R, Gargiulo M, Geraghty P, Goode S, Gray B, Guo W, Gupta PC, Hinchliffe R, Jetty P, Komori K, Lavery L, Liang W, Lookstein R, Menard M, Misra S, Miyata T, Moneta G, Munoa Prado JA, Munoz A, Paolini JE, Patel M, Pompo-

Endothelial progenitor cells and SNAP for limb ischemia

- sellì F, Powell R, Robless P, Rogers L, Schanzer A, Schneider P, Taylor S, De Ceniga MV, Veller M, Vermassen F, Wang J and Wang S; Gvg Writing Group for the Joint Guidelines of the Society for Vascular Surgery (SVS), European Society for Vascular Surgery (ESVS), and World Federation of Vascular Societies (WFVS). Global vascular guidelines on the management of chronic limb-threatening ischemia. *Eur J Vasc Endovasc Surg* 2019; 58: S1-S109, e133.
- [15] Dua A and Lee CJ. Epidemiology of peripheral arterial disease and critical limb ischemia. *Tech Vasc Interv Radiol* 2016; 19: 91-95.
- [16] Lin PY, Sung PH, Chung SY, Hsu SL, Chung WJ, Sheu JJ, Hsueh SK, Chen KH, Wu RW and Yip HK. Hyperbaric oxygen therapy enhanced circulating levels of endothelial progenitor cells and angiogenesis biomarkers, blood flow, in ischemic areas in patients with peripheral arterial occlusive disease. *J Clin Med* 2018; 7: 548.
- [17] Sheu JJ, Lin PY, Sung PH, Chen YC, Leu S, Chen YL, Tsai TH, Chai HT, Chua S, Chang HW, Chung SY, Chen CH, Ko SF and Yip HK. Levels and values of lipoprotein-associated phospholipase A2, galectin-3, RhoA/ROCK, and endothelial progenitor cells in critical limb ischemia: pharmacotherapeutic role of cilostazol and clopidogrel combination therapy. *J Transl Med* 2014; 12: 101.
- [18] Chen YC, Sheu JJ, Chiang JY, Shao PL, Wu SC, Sung PH, Li YC, Chen YL, Huang TH, Chen KH and Yip HK. Circulatory rejuvenated EPCs derived from PAOD patients treated by CD34(+) cells and hyperbaric oxygen therapy salvaged the nude mouse limb against critical ischemia. *Int J Mol Sci* 2020; 21: 7887.
- [19] Hsu SL, Yin TC, Shao PL, Chen KH, Wu RW, Chen CC, Lin PY, Chung SY, Sheu JJ, Sung PH, Chen CY, Wang CJ, Yip HK and Lee MS. Hyperbaric oxygen facilitates the effect of endothelial progenitor cell therapy on improving outcome of rat critical limb ischemia. *Am J Transl Res* 2019; 11: 1948-1964.
- [20] Yeh KH, Sheu JJ, Lin YC, Sun CK, Chang LT, Kao YH, Yen CH, Shao PL, Tsai TH, Chen YL, Chua S, Leu S and Yip HK. Benefit of combined extracorporeal shock wave and bone marrow-derived endothelial progenitor cells in protection against critical limb ischemia in rats. *Crit Care Med* 2012; 40: 169-177.
- [21] Benoit E, O'Donnell TF Jr, Iafrati MD, Asher E, Bandyk DF, Hallett JW, Lumsden AB, Pearl GJ, Roddy SP, Vijayaraghavan K and Patel AN. The role of amputation as an outcome measure in cellular therapy for critical limb ischemia: implications for clinical trial design. *J Transl Med* 2011; 9: 165.
- [22] Kawamura A, Horie T, Tsuda I, Abe Y, Yamada M, Egawa H, Iida J, Sakata H, Onodera K, Tamaki T, Furui H, Kukita K, Meguro J, Yonekawa M and Tanaka S. Clinical study of therapeutic angiogenesis by autologous peripheral blood stem cell (PBSC) transplantation in 92 patients with critically ischemic limbs. *J Artif Organs* 2006; 9: 226-233.
- [23] Liew A, Bhattacharya V, Shaw J and Stansby G. Cell therapy for critical limb ischemia: a meta-analysis of randomized controlled trials. *Angiology* 2016; 67: 444-455.
- [24] Nizankowski R, Petriczek T, Skotnicki A and Szczeklik A. The treatment of advanced chronic lower limb ischaemia with marrow stem cell autotransplantation. *Kardiol Pol* 2005; 63: 351-360; discussion 361.
- [25] Tateishi-Yuyama E, Matsubara H, Murohara T, Ikeda U, Shintani S, Masaki H, Amano K, Kishimoto Y, Yoshimoto K, Akashi H, Shimada K, Iwasaka T and Imaizumi T; Therapeutic Angiogenesis using Cell Transplantation (TACT) Study Investigators. Therapeutic angiogenesis for patients with limb ischaemia by autologous transplantation of bone-marrow cells: a pilot study and a randomised controlled trial. *Lancet* 2002; 360: 427-435.
- [26] Teraa M, Sprengers RW, van der Graaf Y, Peters CE, Moll FL and Verhaar MC. Autologous bone marrow-derived cell therapy in patients with critical limb ischemia: a meta-analysis of randomized controlled clinical trials. *Ann Surg* 2013; 258: 922-929.
- [27] Wang ZX, Li D, Cao JX, Liu YS, Wang M, Zhang XY, Li JL, Wang HB, Liu JL and Xu BL. Efficacy of autologous bone marrow mononuclear cell therapy in patients with peripheral arterial disease. *J Atheroscler Thromb* 2014; 21: 1183-1196.
- [28] Chang CL, Sung PH, Sun CK, Chen CH, Chiang HJ, Huang TH, Chen YL, Zhen YY, Chai HT, Chung SY, Tong MS, Chang HW, Chen HH and Yip HK. Protective effect of melatonin-supported adipose-derived mesenchymal stem cells against small bowel ischemia-reperfusion injury in rat. *J Pineal Res* 2015; 59: 206-220.
- [29] Chen HH, Lin KC, Wallace CG, Chen YT, Yang CC, Leu S, Chen YC, Sun CK, Tsai TH, Chen YL, Chung SY, Chang CL and Yip HK. Additional benefit of combined therapy with melatonin and apoptotic adipose-derived mesenchymal stem cell against sepsis-induced kidney injury. *J Pineal Res* 2014; 57: 16-32.
- [30] Lee FY, Sun CK, Sung PH, Chen KH, Chua S, Sheu JJ, Chung SY, Chai HT, Chen YL, Huang TH, Huang CR, Li YC, Luo CW and Yip HK. Daily melatonin protects the endothelial lineage and functional integrity against the aging process, oxidative stress, and toxic environment and re-

Endothelial progenitor cells and SNAP for limb ischemia

- stores blood flow in critical limb ischemia area in mice. *J Pineal Res* 2018; 65: e12489.
- [31] Manchester LC, Coto-Montes A, Boga JA, Andersen LP, Zhou Z, Galano A, Vriend J, Tan DX and Reiter RJ. Melatonin: an ancient molecule that makes oxygen metabolically tolerable. *J Pineal Res* 2015; 59: 403-419.
- [32] Sun CK, Lee FY, Kao YH, Chiang HJ, Sung PH, Tsai TH, Lin YC, Leu S, Wu YC, Lu HI, Chen YL, Chung SY, Su HL and Yip HK. Systemic combined melatonin-mitochondria treatment improves acute respiratory distress syndrome in the rat. *J Pineal Res* 2015; 58: 137-150.
- [33] Zhang HM and Zhang Y. Melatonin: a well-documented antioxidant with conditional pro-oxidant actions. *J Pineal Res* 2014; 57: 131-146.
- [34] Lin KC, Wallace CG, Yin TC, Sung PH, Chen KH, Lu HI, Chai HT, Chen CH, Chen YL, Li YC, Shao PL, Lee MS, Sheu JJ and Yip HK. Shock wave therapy enhances mitochondrial delivery into target cells and protects against acute respiratory distress syndrome. *Mediators Inflamm* 2018; 2018: 5425346.
- [35] Chang CL, Chen KH, Sung PH, Chiang JY, Huang CR, Chen HH and Yip HK. Combined high energy of extracorporeal shock wave and 5-FU effectively suppressed the proliferation and growth of tongue squamous cell carcinoma. *Biomed Pharmacother* 2021; 142: 112036.
- [36] Brisbois EJ, Handa H, Major TC, Bartlett RH and Meyerhoff ME. Long-term nitric oxide release and elevated temperature stability with S-nitroso-N-acetylpenicillamine (SNAP)-doped Elast-eon E2As polymer. *Biomaterials* 2013; 34: 6957-6966.
- [37] Goudie MJ, Brisbois EJ, Pant J, Thompson A, Potkay JA and Handa H. Characterization of an S-nitroso-N-acetylpenicillamine-based nitric oxide releasing polymer from a translational perspective. *Int J Polym Mater* 2016; 65: 769-778.
- [38] Hopkins SP and Frost MC. Synthesis and characterization of controlled nitric oxide release from S-Nitroso-N-Acetyl-d-Penicillamine covalently linked to polyvinyl chloride (SNAP-PVC). *Bioengineering (Basel)* 2018; 5: 72.
- [39] Oikawa S, Kai Y, Mano A, Nakamura S and Kakimoto Y. A novel nitric oxide donor, S-Nitroso-NPivaloyl-D-penicillamine, activates a non-neuronal cardiac cholinergic system to synthesize acetylcholine and augments cardiac function. *Cell Physiol Biochem* 2019; 52: 922-934.
- [40] Chen YT, Huang KH, Chiang JY, Sung PH, Huang CR, Chu YC, Chuang FC and Yip HK. Extracorporeal shock wave therapy protected the functional and architectural integrity of rodent urinary bladder against ketamine-induced damage. *Biomedicines* 2021; 9: 1391.
- [41] Lee FY, Chen YL, Sung PH, Ma MC, Pei SN, Wu CJ, Yang CH, Fu M, Ko SF, Leu S and Yip HK. Intracoronary transfusion of circulation-derived CD34+ cells improves left ventricular function in patients with end-stage diffuse coronary artery disease unsuitable for coronary intervention. *Crit Care Med* 2015; 43: 2117-2132.